AIP | Applied Physics Letters

Thermal radiation from optically driven Kerr (χ (3)) photonic cavities

Chinmay Khandekar, Zin Lin, and Alejandro W. Rodriguez

Citation: Applied Physics Letters **106**, 151109 (2015); doi: 10.1063/1.4918599
View online: http://dx.doi.org/10.1063/1.4918599
View Table of Contents: http://scitation.aip.org/content/aip/journal/apl/106/15?ver=pdfcov
Published by the AIP Publishing

Thermal radiation from optically driven Kerr ($\chi^{(3)}$) photonic cavities

Chinmay Khandekar,[1] Zin Lin,[2] and Alejandro W. Rodriguez[1]
[1]*Department of Electrical Engineering, Princeton University, Princeton, New Jersey 08540, USA*
[2]*School of Engineering and Applied Sciences, Harvard University, Cambridge, Massachusetts 02139, USA*

(Received 12 March 2015; accepted 7 April 2015; published online 17 April 2015)

We describe thermal radiation from nonlinear ($\chi^{(3)}$) photonic cavities coupled to external channels and subject to incident monochromatic light. Our work extends related work on nonlinear mechanical oscillators to the problem of thermal radiation, demonstrating that bistability can enhance thermal radiation by orders of magnitude and result in strong lineshape alternations, including "super-narrow spectral peaks" occurring at the onset of kinetic phase transitions. We show that when the cavities are designed to exhibit perfect linear emissivity (rate matching), such thermally activated transitions can be exploited to dramatically tune the output power and radiative properties of the cavity, leading to a kind of Kerr-mediated thermo-optic effect. Finally, we demonstrate that in certain parameter regimes, the output radiation exhibits Stokes and anti-Stokes side peaks whose relative magnitudes can be altered by tuning the internal temperature of the cavity relative to its surroundings, a consequence of strong correlations and interference between the emitted and reflected radiation. © *2015 AIP Publishing LLC*. [http://dx.doi.org/10.1063/1.4918599]

Driven nonlinear oscillators, including optical,[1] optomechanical,[2] and MEMS[3,4] resonators, have been studied for decades and exploited for many applications, from mass detection[5] to sensing[6] and tunable filtering.[7] When driven to a non-equilibrium state, these systems can exhibit a wide range of unusual thermal phenomena,[8] leading, for instance, to cooling and amplification of thermal fluctuations in optomechanical systems,[2] generation of squeezed states of light in Kerr media,[9] and stochastic resonances.[10] Previous studies of Duffing oscillators have also identified novel effects arising from the nonlinear interaction of coherent pumps with thermal noise,[11–13] leading to phase transitions and lineshape alterations that were recently observed in a handful of systems, e.g., mechanical oscillators[14,15] and Josephson junctions.[16]

In this letter, we study thermal radiation effects in optically driven $\chi^{(3)}$ photonic cavities coupled to external channels. We demonstrate that in certain parameter regimes, bistability[17,18] in photonic resonators leads to thermally activated transitions that amplify thermal fluctuations by orders of magnitude and cause dramatic changes in the cavity spectrum, analogous to noise-induced switching in mechanical oscillators.[15] We find that when the photonic cavity is critically coupled to the radiation channel (enforced by designing the cavity to have equal dissipation and radiation rates),[19] the coherent part of the output power varies dramatically with temperature, leading to a kind of Kerr-mediated thermo-optic effect. A simple perturbative analysis also shows that outside of the bistability region, the interaction of the coherent drive with thermal noise leads to amplified, Raman-type Stokes and anti-Stokes side peaks in the radiation spectrum, the relative amplitudes of which depend on a sensitive interference between the externally incident and reflected thermal radiation. Related phenomena have been predicted[13] and more recently observed[14,15] in the context of driven nonlinear mechanical oscillators as well as resonators based on rf-driven Josephson junctions,[16] and microscopic theories have also been used to describe related optical effects in the quantum regime.[20] Our work is an extension of these studies to the particular problem of thermal radiation from photonic resonators. As we show below, additional considerations arising in the case of radiation from cavities but absent in mechanical oscillators or bulk media, such as the strong coupling of the cavity to an external channel, dramatically impact the outgoing radiation. The ability to tune the radiation properties of resonators via temperature and optical signals offers potentially new avenues for applications in nano-scale heat regulation,[21] detection,[22] rectification,[23,24] photovoltaics,[25] and incoherent sources.[26] We propose a practical photonic structure where these effects can arise near room temperature and at mW powers.

The system under consideration belongs to the class of nonlinear photonic resonators depicted in Fig. 1, involving a cavity coupled to an external channel (e.g., a waveguide). The description of thermal radiation in this system can be carried out via the coupled-mode theory framework,[27] which we recently employed to study thermal radiation in a related system[28] but now extend to consider the addition of a coherent pump. The equations describing the cavity mode a are given by[28]

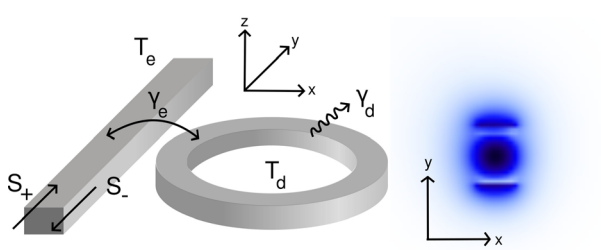

FIG. 1. Schematic of a wavelength-scale silicon ring resonator of radius $R = 4.4$ μm, height $h = 220$ nm, and width $w = 350$ nm, coupled to a silicon waveguide (channel), both on a silica substrate. Also shown is the E_y mode profile of a resonance designed to have azithmutal number $m = 25$, wavelength $\lambda = 1.5$ μm, radiative lifetimes $\gtrsim 10^6$, and relatively large nonlinear coupling coefficient $\alpha = 0.032\chi^{(3)}\omega_0/(8\epsilon_0\lambda^3)$. The loss γ_d and waveguide–coupling γ_e rates are much larger than the corresponding radiation rate.

$$\frac{da}{dt} = \left[i\left(\omega_0 - \alpha|a|^2\right) - \gamma\right]a + \sqrt{2\gamma_d}\xi_d + \sqrt{2\gamma_e}s_+, \quad (1)$$

$$s_- = -s_+ + \sqrt{2\gamma_e}a, \quad (2)$$

where $|a|^2$ is the energy of the cavity mode and $|s_\pm|^2$ are the incident (+) and outgoing (−) power from and into the external channel, respectively. The latter arises due to dissipative noise inside the cavity ξ_d as well as externally incident light s_+ consisting of both thermal radiation ξ_e and a monochromatic pump $s_p \exp(i\omega_p t)$. The dynamics of the cavity field are described by its resonance frequency ω_0 and decay rate $\gamma = \gamma_e + \gamma_d$, which includes linear absorption γ_d as well as decay into the external channel γ_e. The real and imaginary parts of the nonlinear coefficient $\alpha = \frac{3}{4}\omega_0 \int \varepsilon_0 \chi^{(3)}|\vec{E}|^4 / (\int \varepsilon|\vec{E}|^2)^2$ depend on a complicated overlap integral of the linear cavity fields,[29] and lead to self-phase modulation (SPM) and two-photon absorption (TPA), respectively. We mainly focus on the effects of SPM (real $\alpha > 0$), since we find that TPA leads to thermal broadening of the kind explored in Ref. 28. Both internal and external thermal sources are represented by stochastic, delta-correlated white-noise sources ξ_e and ξ_d satisfying (assuming $\gamma \ll \omega_0$),

$$\langle \xi^*(t)\xi(t')\rangle = \Theta(\omega_0, T)\delta(t - t'), \quad (3)$$

where $\langle \ldots \rangle$ denotes a thermodynamic or ensemble average and $\Theta(\omega, T) = \hbar\omega/(e^{\hbar\omega/k_B T} - 1)$ is the mean energy of a Planck oscillator[23] at local temperature T; the temperatures of the internal and external baths are denoted as T_d and T_e, respectively. Above, we assumed $\hbar\gamma/k_B \ll T_e, T_d$ allowing us to ignore the frequency-dispersion and temporal correlations (colored noise) associated with Θ. (Note that in the limit $\hbar\omega_0/k_B T \to 0$ one obtains the classical result $\Theta \to k_B T$.)

Thermal amplification and power tunability—We show that bistability can amplify thermal fluctuations and lead to enhanced, temperature-tunable emission from the cavity. We begin by reviewing a number of key features of the system in the absence of thermal noise, whose contributions are considered perturbatively due to the generally weak nature of thermal noise, i.e., $|s_p|^2 \gg \gamma k_B T$. The steady-state field a_0 due to the pump is given by the well-known cubic equation[13,30]

$$\left[\left(\Delta + \frac{\alpha|a_0|^2}{\gamma}\right)^2 + 1\right]\frac{\alpha|a_0|^2}{\gamma} = 2\zeta, \quad (4)$$

where $\zeta \equiv \alpha|s_p|^2\gamma_e/\gamma^3$ is the effective nonlinear coupling associated with the pump and $\Delta \equiv \frac{\omega_p - \omega_0}{\gamma}$ is the dimensionless detuning. Equation (4) describes a number of extensively studied nonlinear effects,[30,31] including bistability arising in the regime $\Delta < -\sqrt{3}$ and $\zeta^{(1)} < \zeta < \zeta^{(2)}$, as illustrated by the hysteresis plot on the inset of Fig. 2(a), which shows the dimensionless cavity energy $x = \alpha|a|^2/\gamma$ as a function of ζ.

An effect that seems little explored but that plays an important role on the thermal properties of this system is perfect absorption, which occurs when a photonic cavity is driven on resonance and its dissipation and radiation rates are equal, also known as rate matching.[19] In the presence of nonlinearities, the cavity frequency and hence the absorbed power depend on ζ. For instance, in the non-bistable regime, the output power varies slowly with ζ, as illustrated by the green curve in Fig. 2(a) for $\Delta = -1$, increasing and then decreasing as $\zeta \to |\Delta/2|$, at which point the cavity and pump frequencies are in resonance, i.e., $\alpha|a_0|^2/\gamma = -\Delta$. Bistability can lead to a more pronounced dependence on ζ: the two stable steady states experience different frequency shifts and hence loss rates, and ultimately which state is excited in the steady state depends on the specific initial (or excitation) conditions.[32] Figure 2(a) shows the steady-state output power $|s_-|^2$ as ζ is adiabatically increased (solid lines) from zero and beyond the critical point $\zeta^{(2)}$, for multiple Δ. Similarly, the dashed blue line shows the power as ζ is adiabatically decreased below $\zeta^{(2)}$ for the particular case

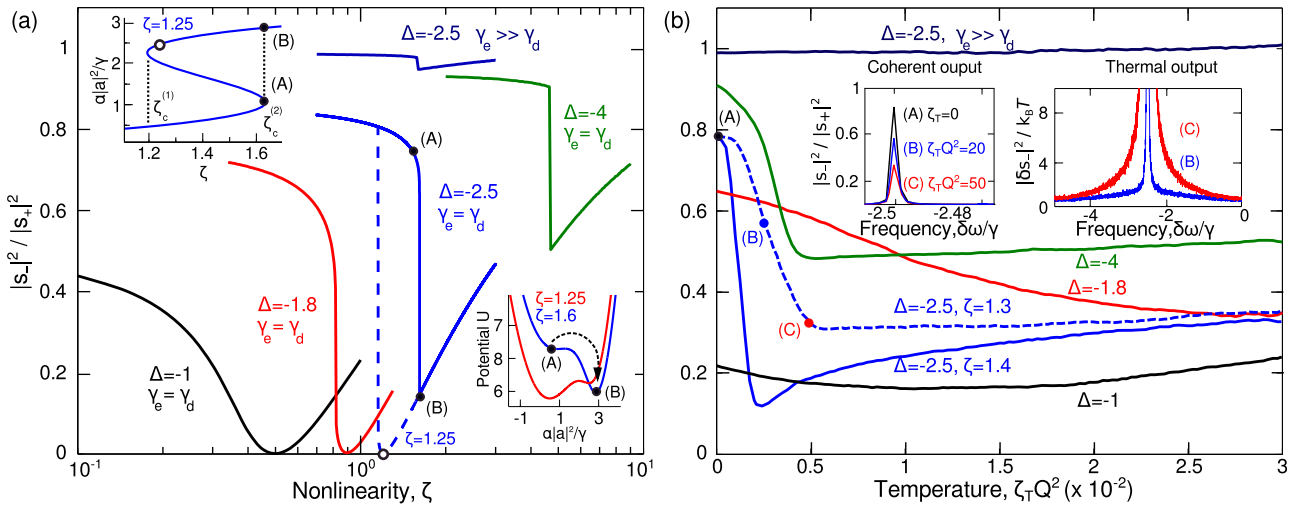

FIG. 2. (a) Output power $\langle|s_-|^2\rangle$ normalized by the input power $\langle|s_+|^2\rangle$ of the pumped system described in Fig. 1, in the absence of thermal noise and as a function of ζ, for different values of detuning $\Delta = \frac{\omega_p - \omega_0}{\gamma}$. The top left inset shows a hysteresis plot of the energy $\alpha|a_0|^2/\gamma$ as a function of ζ, the solutions of (4), for the particular choice of $\Delta = -2.5$, while the bottom inset shows the corresponding potential energy U as a function of the cavity energy for two different $\zeta = |\Delta/2|$ and $\zeta^{(2)}$. (b) The same normalized output power $\langle|s_-|^2\rangle/\langle|s_+|^2\rangle$ as a function of temperature $\zeta_T Q^2$, where $\zeta_T = \alpha\Theta(\omega_0, T)\gamma_e/\gamma^2$ and $Q = \omega_0/\gamma$, for different values of Δ and $\zeta \lesssim \zeta^{(2)}$. The insets illustrate the change in the coherent (left) and thermal radiation (right) spectra. Both internal and external baths have equal temperatures $T_d = T_e = T$.

$\Delta = -2.5$, demonstrating that only the upper branch experiences perfect absorption, occurring at $\zeta = |\Delta/2|$ and marked by the white circle. The corresponding change in the output power as the system transitions from the lower (A) to the higher (B) energy state at $\zeta^{(2)}$ is given approximately by

$$|s_+|^2\left(1-\frac{\gamma_e-\gamma_d}{\gamma_e+\gamma_d}\right)\frac{(\Delta+x_1)^2-(\Delta+x_2)^2}{\left[1+(\Delta+x_1)^2\right]\left[1+(\Delta+x_2)^2\right]}, \quad (5)$$

where $x_1 = -\frac{1}{3}(2\Delta + \sqrt{\Delta^2-3})$ and $x_2 = -2(\Delta+x_1)$ are the cavity energies associated with the lower and higher energy states, respectively. Given (5), one can show that the difference in output power is largest under the rate matching condition $\gamma_e = \gamma_d$ and at $\Delta \approx -7/3$, decreasing with smaller or larger detuning.

The presence of noise complicates this picture due to finite–temperature fluctuations which cause the system to undergo transitions between the two states, where the rates of forward/backward transitions are a complicated function of the potential energy U and temperature of the system.[13,32] As described in Ref. 33, U is obtained by integrating the steady-state equation associated with the cavity energy $\frac{dx}{dt} = \frac{4\gamma\zeta}{(\Delta+x)^2+1} - 2\gamma x$ with respect to $x = \alpha|a|^2/\gamma$. Examples of U are shown on the lower inset of Fig. 2(a) for two values of ζ. Thermally activated hopping leads to significant enhancement of amplitude fluctuations, which manifest as large changes in the radiation spectrum of the cavity. This is illustrated by the top inset of Fig. 2(b), which shows the thermal outgoing power $\langle|\delta s_-(\omega)|^2\rangle$ for the particular choice of $\Delta = -2.5$ and $\zeta = 1.3$ and for multiple values of $\zeta_T Q^2$, where for convenience (below) we have introduced the dimensionless effective thermal coupling $\zeta_T \equiv \alpha\Theta(\omega_0, T)\gamma_e/\gamma^2$ and cavity-lifetime $Q = \omega_0/\gamma$.[19] Here, the thermal radiation $\langle|\delta s_-|^2\rangle = \langle|s_-|^2\rangle - |\langle s_-\rangle|^2$ is obtained by subtracting the coherent from the total output power. Such enhancements in thermal fluctuations were predicted to occur and recently observed in nonlinear mechanical oscillators,[13,14] where at special ζ the oscillators were shown to undergo a so-called kinetic phase transition associated with equal rates of forward/backward hopping, leading to "supernarrow" and highly amplified spectral peaks. Interestingly, we find that in the case of optical resonators, thermal amplification can be accompanied by a significant decrease in the coherent output power despite the fact that $|s_p|^2 \gg \gamma k_B T$, a consequence of perfect absorption. In particular, operating under rate matching and near $\zeta^{(2)}$ allows for temperature to initiate transitions (A)$\rightleftharpoons$(B), leading to significant changes in $\langle|s_-|^2\rangle$ with respect to T. Essentially, as $\zeta \to \zeta^{(2)}$, the potential barrier separating the lower x_1 from the higher x_2 energy states begins to disappear, resulting in increased rate of forward transitions and hence larger absorption.

These features are illustrated in Fig. 2(b), which shows the total output power as a function of $\zeta_T Q^2$ for different combinations of ζ and Δ. (We found numerically that for a given ζ and Δ, changing either ζ_T or Q^2 while leaving $\zeta_T Q^2$ unchanged leaves the relative output power unaltered.) Noticeably, while the change in the output power is gradual in the non-bistable regime ($\Delta > -\sqrt{3}$), there is a significantly stronger dependence in the bistable regime, with the slope becoming increasingly sharper as $\zeta \to \zeta^{(2)}$ and $\zeta_T \to 0$ as it becomes increasingly easier for lower T fluctuations to induce hopping unto the higher-energy state. At sufficiently large ζ_T, $\langle|s_-|^2\rangle$ is found to increase with increasing ζ_T as the cavity field no longer probes the hysteresis regime. While the maximum change in $\langle|s_-|^2\rangle$ can be estimated from the steady-state analysis in the absence of noise (with the largest change occurring for $\Delta \approx -7/3$), its dependence on ζ_T is a complicated function of ζ and Δ. For instance, for $\Delta = -2.5$ and $\zeta = 1.4$ [blue line in Fig. 2(b)], the sharp decrease in output power occurs at $\zeta_T Q^2 \approx 10$ and yields a slope $\frac{1}{|s_+|^2}\frac{\delta(|s_-|^2)}{\delta(\zeta_T Q^2)} \approx 0.05$.

Side peaks—The radiation spectrum also exhibits other interesting features, including the emergence of Raman-type Stokes and anti-Stokes side peaks previously observed in driven mechanical oscillators.[13,14] Interestingly, we find that in our photonic resonator, the presence of the external channel dramatically alters the relative amplitudes of the side peaks, e.g., leading to a symmetric spectrum when the two baths have equal temperatures. We begin by exploiting a simple perturbation theory in which the thermal fluctuations of the cavity-field δa and radiation $\delta s_- = -\xi_e + \sqrt{2\gamma_e}\delta a$ are treated perturbatively, leading to analytical expressions for the corresponding thermal energy and radiation spectra.[33] Assuming $|s_p|^2 \gg \gamma k_B\{T_d, T_e\}$, we obtain

$$\langle|\delta a|^2\rangle = \frac{k_B f_+(2\gamma_d T_d + 2\gamma_e T_e)}{D}, \quad (6)$$

$$\langle|\delta s_-|^2\rangle = k_B T_e + \frac{4\gamma_e k_B}{D}[\gamma_d(f_+ T_d - f_- T_e) + \gamma_e(f_+ - f_-)T_e], \quad (7)$$

where f_+, f_- and D are given by

$$f_\pm = (\omega + \omega_0 - 2\omega_p - 2\alpha|a_0|^2)^2 + \gamma^2 \pm \alpha^2|a_0|^4$$
$$D = [\gamma^2 + (\omega_0 - \omega_p - 2\alpha|a_0|^2)^2 - (\omega-\omega_p)^2 - \alpha^2|a_0|^4]^2 + 4\gamma^2(\omega-\omega_p)^2,$$

and where $|a_0|^2$ denotes the steady-state cavity energy in the absence of fluctuations, i.e., the solution of (4). Note that for simplicity we assumed the classical limit $\Theta(\omega_0, T) \to k_B T$. In the absence of the external bath $T_e = 0$, the above equations are similar to those obtained in the case of mechanical oscillators.[13] However, the situation changes in the presence of the channel due to interference and induced correlations between the emitted and reflected radiation, described in (7) by the f_- terms.

Figure 3 illustrates the radiation spectrum of the cavity under different operating conditions, showing excellent agreement between the numerically (noisy) and analytically (dashed lines) computed spectra. We note that all of the results shown in Fig. 3 correspond to cavities operating outside of the bistable regime: although it is possible to obtain a complete and analytical description of the spectrum based on (6) and (7), such an analysis is more difficult in the bistable regime due to hopping between states, requiring a complicated description of the transition rates and stationary distributions of the system.[13] For instance, in the bistable regime,

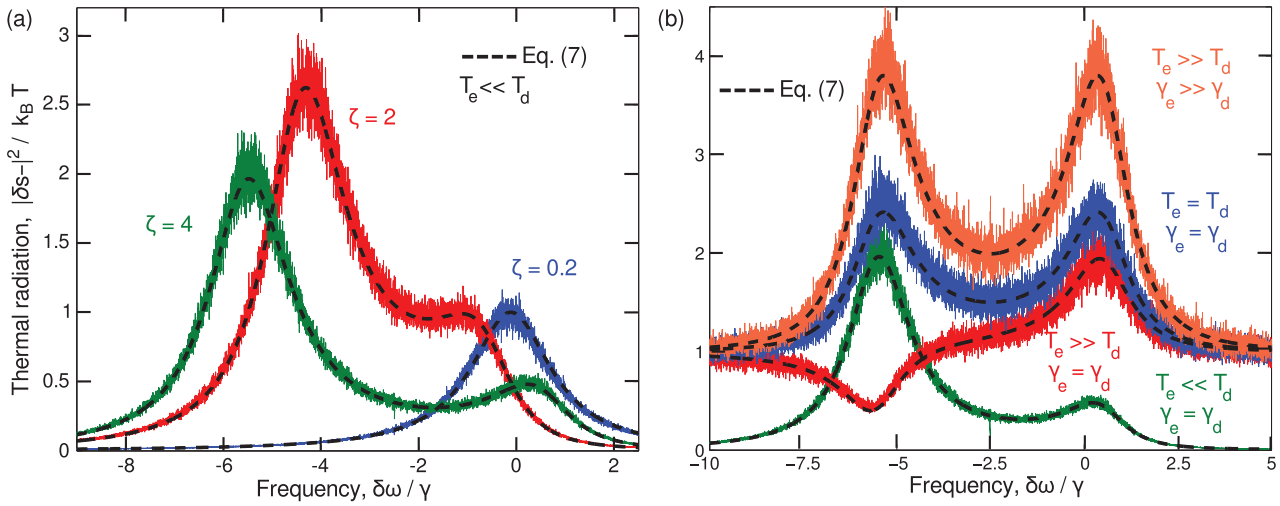

FIG. 3. Thermal radiation $|\delta s_-|^2$ for the system described in Fig. 1, normalized by the maximum of the internal and external bath temperatures $T = \max\{T_d, T_e\}$, as a function of the dimensionless frequency $\delta\omega/\gamma$ where $\delta\omega = (\omega - \omega_0)$, with fixed $\Delta = -2.5$ and under various operating conditions. The radiation spectrum is shown (a) in the limit $T_d \gg T_e$ of negligible externally incident radiation, for different values of ζ and (b) for fixed $\zeta = 4$ but different T_d, T_e and linear decay rates γ_d and γ_e.

the system exhibits a temperature-dependent supernarrow spectral peak whose amplitude decreases with increasing ζ. In the absence of bistability, a similar but weaker amplification occurs as $\zeta \to |\Delta/2|$ or equivalently, as the cavity frequency becomes resonant with the pump. Regardless of regime, at sufficiently large ζ (once the cavity resonance has crossed ω_p), modulation of the thermal noise by the pump causes the spectrum to transition from being singly to doubly resonant due to the emergence of an additional anti-Stokes peak.[13] In the limit as $\zeta \to \infty$, both peaks move farther apart and their amplitudes asymptote to a parameter-dependent constant.

Figure 3(b) explores the dependence of the peak amplitudes on various cavity parameters, including $T_d = T_e$, $T_d \gg T_e$, and $T_d \ll T_e$, corresponding to a resonator that is either at thermal equilibrium, heated, or cooled with respect to its surroundings, respectively. When noise entering the system through the external bath is negligible $T_d \gg T_e$, similar to the previously explored situation involving mechanical oscillators,[13] one finds that the Stokes peak is always much larger than the anti-Stokes peak (green line). Essentially, for $\alpha > 0$ the cavity nonlinearity favors down-conversion, as captured by the asymmetric f_+ terms above. The peak radiation associated with the Stokes peak can be readily obtained from (6) in the non-bistable regime $\Delta \leq -\sqrt{3}$, and is given by $\max|\delta s_-|^2 = \frac{4\gamma_e\gamma_d}{\gamma^2}\left(1 + 2\Delta^2\right)k_B T_d$, reaching $7k_B T_d$ precisely at the onset of bistability and when $\gamma_e = \gamma_d$. Note that due to the rate matching condition, the coherent pump is completely absorbed in this limit and thus only thermal radiation is observed at the output of the channel. At larger $\zeta > |\Delta/2|$, the amplitude of both peaks decreases with increasing ζ where, as $\zeta \to \infty$ (not shown), the amplitude of the Stokes peak $\to k_B T_d$ while the anti-Stokes peak disappears. The situation changes dramatically when the noise entering the system through the external bath cannot be ignored, i.e., $T_e \gtrsim T_d$. In particular, as observed from (6), although the cavity spectrum favors Stokes to anti-Stokes conversion regardless of the relative temperatures or decay rates, we find that the spectrum of outgoing radiation can be dramatically different depending on the regime of operation. When $T_e \gg T_d$ where noise is dominated by external radiation, we find that the anti-Stokes peak dominates (red line) except when $\gamma_e \gg \gamma_d$, at which point the spectrum exhibits a symmetric lineshape (orange line). Such a reversal in relative amplitudes is captured by the f_- terms above, which include correlations and interference between the emitted and reflected radiation. The maximum radiation in the non-bistable regime in this case $\max|\delta s_-|^2 = k_B T_e\left(1 + \frac{8\gamma_e^2}{\gamma^2}\Delta^2 - \frac{4\gamma_e\gamma_d}{\gamma^2}\right)$, reaching $25k_B T_e$ at the onset of bistability and when $\gamma_e \gg \gamma_d$ (rather than under rate matching). Interestingly, we find that when the two baths lie at the same temperature $T_e = T_d$, both peaks have equal amplitudes regardless of γ_e/γ_d, though the maximum amplitude in this regime also occurs in the limit $\gamma_e \gg \gamma_d$. This unexpected symmetrization of the spectrum arising due to interference effects seems to be unique to this particular system. Previous work on nonlinear electromagnetic fluctuations in the quantum regime observed similar peaks in the spectrum, but in that case a symmetric spectrum was obtained only at zero temperature (a singular point of the theory[34]) due to quantum tunneling.[20]

Although a number of the abovementioned effects have been observed in mechanical oscillators, they remain unobserved in the context of thermal radiation where they could potentially be exploited in numerous applications.[21,25,26] As demonstrated above, the interplay between the internal and externally incident radiation and the coherent pump leads to new effects in thermal radiators, including dramatic changes in both the coherent and thermal output spectrum with temperature, along with temperature–tunable Stokes and anti-Stokes side peaks. Finally, we conclude by proposing a realistic, silicon ring resonator design, depicted schematically in Fig. 1, where one could potentially observe these effects near room temperature and with operating $Q \sim 10^5$ and input power $|s_p|^2 \sim 1\text{mW}$, in which case $\alpha|s_p|^2 Q^2 \sim |\Delta|$. For these parameters, we find that $\frac{1}{|s_+|^2}\frac{\delta(|s_-|^2)}{\delta(T)} \sim 0.04\text{K}^{-1}$ at $T \approx 300\,\text{K}$.

Although this is almost two orders of magnitude smaller in comparison with thermo-optic effects in silicon, which lead to tunable powers $\sim K^{-1}$ for the same structure, at lower temperatures $T \lesssim 100\,K$ where the thermo-optic coefficient is much smaller,[35] our fluctuation-induced effects offer significantly better temperature tunability. Other cavity designs such as the nanobeam cavity described in Ref. 36 yield much larger α and allow smaller Q to be employed, leading to greater tunability compared to that obtained from thermo-optic effects.

We are grateful to Mark Dykman for very helpful comments and suggestions. This work was supported in part by the National Science Foundation under Grant No. DMR-1454836.

[1]K. J. Vahala, "Optical microcavities," Nature **424**, 839–846 (2003).
[2]T. J. Kippenberg and K. J. Vahala, "Cavity opto-mechanics," Opt. Express **15**(25), 17172–17205 (2007).
[3]R. Lifshitz and M. C. Cross, "Nonlinear dynamics of nanomechanical and micromechanical resonators," Rev. Nonlinear Dyn. Complexity **1**, 1–50 (2008).
[4]R. Quidant, J. Gieseler, and L. Novotny, "Thermal nonlinearities in a nanomechanical oscillator," Nat. Phys. **9**, 806–810 (2013).
[5]J. Chaste, A. Eichler, J. Moser, G. Cellabos, R. Rurali, and A. Bachtold, "A nanomechanical mass sensor with yoctogram resolution," Nat. Nanotechnol. **7**, 301–304 (2012).
[6]A. N. Clelan and M. L. Roukes, "Noise processes in nanomechanical resonators," J. Appl. Phys. **92**(5), 2758–2769 (2002).
[7]R. Almog, S. Zaitsev, O. Shtempluck, and E. Buks, "High intermodulation gain in a micromechanical duffing resonator," Appl. Phys. Lett. **88**, 213509 (2006).
[8]*Fluctuating Nonlinear Oscillators: From Nanomechanics to Quantum Superconducting Circuits*, edited by M. Dykman (Oxford University Press, 2012), Chap. 13.
[9]L.-A. Wu, M. Xiao, and H. J. Kimble, "Squeezed states of light from an optical parametric oscillator," JOSA-B **4**, 1465–1476 (1987).
[10]L. Gammaltoni, P. Hangi, P. Jung, and F. Marchesonl, "Stochastic resonance," Rev. Mod. Phys. **70**, 223 (1998).
[11]M. I. Dykman, "Theory of nonlinear nonequilibrium oscillators interacting with a medium," Zh. Eksp. Theor. Fiz. **68**, 2082–2094 (1975).
[12]M. I. Dykman and P. V. E. McClintok, "Power spectra of noise-driven nonlinear systems and stochastic resonance," Physica D **58**, 10–30 (1992).
[13]M. I. Dykman, D. G. Luchinsky, and R. Manella, "Supernarrow spectral peaks and high-frequency stochastic resonance in systems with coexisting periodic attractors," Phys. Rev. E **49**(2), 1198–1215 (1994).
[14]C. Stambaugh and H. B. Chan, "Supernarrow spectral peaks near a kinetic phase transition in a driven nonlinear micromechanical oscillator," Phys. Rev. Lett. **97**, 110602 (2006).
[15]C. Stambaugh and H. B. Chan, "Noise-activated switching in a driven nonlinear micromechanical oscillator," Phys. Rev. B **73**, 172302 (2006).
[16]S. Andre, L. Guo, V. Peano, M. Mathaler, and G. Schon, "Emission spectrum of the driven nonlinear oscillator," Phys. Rev. A **85**, 053825 (2012).
[17]M. Notomi, A. Shinya, S. Mitsugi, G. Kira, E. Kuramochi, and T. Tanabe, "Optical bistable switching action of Si high-q photonic-crystal nanocavities," Opt. Express **13**(7), 2678–2687 (2005).
[18]A. R. Cowan and J. F. Young, "Optical bistability involving photonic crystal microcavities and fano line shapes," Phys. Rev. E **68**, 046606 (2003).
[19]J. D. Joannopoulos, S. G. Johnson, J. N. Winn, and R. D. Meade, *Photonic Crystals: Molding the Flow of Light*, 2nd ed. (Princeton University Press, 2008).
[20]P. D. Drummond and D. F. Walls, "Quantum theory of optical bistability. I. Nonlinear polarisability model," J. Phys. A **13**, 725 (1980).
[21]L. Wang and B. Li, "Thermal memory: A storage of phononic information," Phys. Rev. Lett. **101**, 267203 (2008).
[22]K. Nozaki, S. Matsuo, K. Takeda, T. Sato, E. Kuramochi, and M. Notomi, "Ingaas nano-photodetectors based on photonic crystal waveguide including ultracompact buried heterostructure," Opt. Express **21**, 19022 (2013).
[23]C. R. Otey, W. T. Lau, and S. Fan, "Thermal rectification through vacuum," Phys. Rev. Lett. **104**(15), 154301 (2010).
[24]N. A. Roberts and D. G. Walker, "A review of thermal rectification observations and models in solid materials," J. Therm. Sci. **50**, 648–662 (2011).
[25]A. Lenert, D. M. Bierman, Y. Nam, W. R. Chan, I. Celanovic, M. Soljacic, and E. N. Wang, "A nanophotonic solar thermophotovoltaic device," Nat. Nanotechnol. **9**, 126–130 (2014).
[26]S. Noda, M. Fujita, and T. Asano, "Spontaneous-emission control by photonic crystals and nanocavities," Nat. Photonics **1**, 449–458 (2007).
[27]H. A. Haus, *Waves and Fields in Optoelectronics* (Prentice-Hall, Englewood Cliffs, NJ, 1984), Chap. 7.
[28]C. Khandekar, A. Pick, S. G. Johnson, and A. W. Rodriguez, "Radiative heat transfer in nonlinear Kerr media," Phys. Rev. B **91**, 115406 (2015).
[29]A. Rodriguez, M. Soljačić, J. D. Joannopoulos, and S. G. Johnson, "$\chi^{(2)}$ and $\chi^{(3)}$ harmonic generation at a critical power in inhomogeneous doubly resonant cavities," Opt. Express **15**(12), 7303–7318 (2007).
[30]M. Soljacic, M. Ibanescu, S. J. Johnson, Y. Fink, and J. D. Joannopoulos, "Optimal bistable switching in nonlinear photonic crystals," Phys. Rev. E **66**, 055601 (2002).
[31]S. G. Johnson, A. Mekis, S. Fan, and J. D. Joannopoulos, "Molding the flow of light," Comput. Sci. Eng. **3**(6), 38–47 (2001).
[32]S. H. Strogatz, *Nonlinear Dynamics and Chaos* (Westview Press, Boulder, CO, 1994).
[33]See supplementary material at http://dx.doi.org/10.1063/1.4918599 for the derivation of potential energy function and the perturbative expressions for the thermal energy and radiation spectra.
[34]M. I. Dykman and M. A. Krivoglaz, "Theory of nonlinear oscillators interacting with a medium," Sov. Phys. Rev. **5**, 265–441 (1984).
[35]J. Komma, C. Schwarz, G. Hoffman, D. Heinert, and R. Nawrodt, "Thermo-optic coefficient of silicon at 1550 nm and cryogenic temperatures," Appl. Phys. Lett. **101**, 041905 (2012).
[36]P. B. Deotare, M. W. McCutcheon, I. W. Frank, M. Khan, and M. Loncar, "High quality factor photonic crystal nanobeam cavities," Appl. Phys. Lett. **94**, 121106 (2009).